Biosci. Rep. (2013) / **33** / art:e00026 / doi 10.1042/BSR20120123

OPEN ACCESS

Original Paper

Bioscience Reports

www.bioscirep.org

Bioscience Reports

ALG-2-interacting Tubby-like protein superfamily member PLSCR3 is secreted by an exosomal pathway and taken up by recipient cultured cells

Tatsutoshi INUZUKA*, Akira INOKAWA*, Cen CHEN*, Kumiko KIZU†, Hiroshi NARITA†, Hideki SHIBATA* and Masatoshi MAKI*[1]

*Department of Applied Molecular Biosciences, Graduate School of Bioagricultural Sciences, Nagoya University, Furo-cho, Chikusa-ku, Nagoya 464-8601, Japan, and †Department of Food and Nutrition, Kyoto Women's University, 35 Kitahiyoshi-cho, Imakumano, Higashiyama-ku, Kyoto 605-8501, Japan

Synopsis

PLSCRs (phospholipid scramblases) are palmitoylated membrane-associating proteins. Regardless of the given names, their physiological functions are not clear and thought to be unrelated to phospholipid scrambling activities observed *in vitro*. Using a previously established cell line of HEK-293 (human embryonic kidney-293) cells constitutively expressing human Scr3 (PLSCR3) that interacts with ALG-2 (apoptosis-linked gene 2) Ca^{2+}-dependently, we found that Scr3 was secreted into the culture medium. Secretion of Scr3 was suppressed by 2-BP (2-bromopalmitate, a palmitoylation inhibitor) and by GW4869 (an inhibitor of ceramide synthesis). Secreted Scr3 was recovered in exosomal fractions by sucrose density gradient centrifugation. Palmitoylation sites and the N-terminal Pro-rich region were necessary for efficient secretion, but ABSs (ALG-2-binding sites) were dispensable. Overexpression of GFP (green fluorescent protein)-fused $VPS4B^{E235Q}$, a dominant negative mutant of an AAA (ATPase associated with various cellular activities) ATPase with a defect in disassembling ESCRT (endosomal sorting complex required for transport)-III subunits, significantly reduced secretion of Scr3. Immunofluorescence microscopic analyses showed that Scr3 was largely localized to enlarged endosomes induced by overexpression of a GFP-fused constitutive active mutant of Rab5A (GFP–$Rab5A^{Q79L}$). Secreted Scr3 was taken up by HeLa cells, suggesting that Scr3 functions as a cell-to-cell transferable modulator carried by exosomes in a paracrine manner.

Key words: apoptosis-linked gene 2 (ALG-2), endosome, exosome, palmitoylation, unconventional secretion, vesicle

Cite this article as: Inuzuka, T., Inokawa, A., Chen, C., Kizu, K., Narita, H., Shibata, H. and Maki, M. (2013) ALG-2-interacting Tubby-like protein superfamily member PLSCR3 is secreted by exosomal pathway and taken up by recipient cultured cells. Biosci. Rep. **33**(2), art:e00026.doi:10.1042/BSR20120123

INTRODUCTION

PLSCR (phospholipid scramblase) is engaged in bidirectional translocation of phospholipids (scrambling) between the inner and outer leaflets of biological membranes to collapse the asymmetrical phospholipid distribution. The name PLSCR was assigned to a factor that was first isolated from human erythrocyte membranes and which was shown to possess such a Ca^{2+}-dependent scrambling activity *in vitro* and predicted to be a type II transmembrane protein containing a hydrophobic α-helix in the C-terminal region [1,2]. Subsequent studies, however, have shown that Scr1 (PLSCR1) displays apparently phospholipid scrambling-independent behaviours, such as translocation to the nucleus to function as a transcription factor with a DNA-binding ability and regulation of transacting activity of HTLV-1 (human T-cell leukaemia virus 1) Tax [3–6]. Blood cells from Scr1-deficient mice (*Plscr1*$^{-/-}$) exhibited normal phosphatidylserine mobilization to the cell surface upon stimulation but defective haematopoietic response to growth factors [7]. Accumulating data suggest that Scr1 functions in signal transduction pathways by physically associating with either membrane surface receptors or Src family kinases [8–12]. Since the eight-transmembrane protein TMEM16F has been discovered as a genuine Ca^{2+}-dependent

Abbreviations used: AAA, ATPase associated with various cellular activities; ABS, ALG-2-binding site; ALG-2, apoptosis-linked gene 2; Alix, ALG-2-interacting protein X; ARRDC1, arrestin domain-containing protein 1; 2-BP, 2-bromopalmitate; CM, conditioned medium; DPMB, direct plasma membrane budding; ECM1, extracellular matrix protein 1; EGFP, enhanced green fluorescent protein; ER, endoplasmic reticulum; ESCRT, endosomal sorting complex required for transport; GAPDH, glyceraldehyde-3-phosphate dehydrogenase; GFP, green fluorescent protein; HEK, human embryonic kidney; HPβCD, 2-hydroxypropyl-β-cyclodextrin; ILV, intraluminal vesicle; LC–MS/MS, liquid chromatography–tandem MS; mAb, monoclonal antibody; MVB, multivesicular body; MVE, multivesicular endosome; nSMase, neutral sphingomyelinase; pAb, polyclonal antibody; PLSCR, phospholipid scramblase; TCL, total cell lysate; TULP, Tubby-like protein; WB, Western blotting; WT, wild-type.

[1] To whom correspondence should be addressed (email: mmaki@agr.nagoya-u.ac.jp).

scrambling factor working *in vivo* [13,14], physiological functions of Scr1 are presumed to be unrelated to the phospholipid scrambling activity observed in *in vitro* experiments (see [15,16] for reviews). In mammalian genomes, five 'phospholipid scramblase' paralogues (*PLSCR1–5*) have been identified (*PLSCR1–4* reported in [17]; *PLSCR5* annotated in the NCBI database, NP_001078889.1). Scr3 is involved in transport and synthesis of cardiolipin in mitochondria and in promotion of apoptosis [18–21]. Disruption of the Scr3 gene in mice (*Plscr3*$^{-/-}$) resulted in aberrant accumulation of abdominal fat in adult mice accompanying insulin resistance, glucose intolerance and dyslipidaemia [22]. We previously identified Scr3 as a protein interacting with ALG-2 (apoptosis-linked gene 2), a penta-EF-hand Ca^{2+}-binding protein [23,24]. ALG-2 binds Ca^{2+}-dependently to two distinct sites in the N-terminal Pro-rich region that was less conserved with other Scr family members.

Bioinformatical structure modelling of Scr1 based on known 3D (three-dimensional) structures in the protein database has suggested that PLSCRs are similar to Tubby and TULPs (Tubby-like proteins) and constitute a new superfamily of proteins with a domain containing a β-barrel enclosing a central α-helix [25]. Indeed, we found that Scr3 also has a similar predicted 3D structure (Supplementary Figure S1 at http://www.bioscirep.org/bsr/033/bsr033e026add.htm), and the type II transmembrane hypothesis needs to be corrected. While PLSCRs are palmitoylated for membrane anchoring [3], TULPs are tethered to membranes by binding to phosphatidylinositol 4,5-bisphosphate [26,27]. TULP1 and Scr1, both of which have no signal peptide sequence, are secreted to the extracellular space by a mechanism different from the conventional ER (endoplasmic reticulum)–Golgi pathway, and they bind to the MerTK receptor for phagocytosis and to ECM1 (extracellular matrix protein 1) in HaCaT keratinocytes, respectively [28–30]. Although secretion of Scr1 is abrogated by depletion of membrane cholesterol and has been suggested to occur via a lipid raft-dependent mechanism, the secretory mechanisms are not yet clear. We previously established a cell line of HEK (human embryonic kidney)-293 cells that constitutively express the Scr3 protein [24]. Using this cell line, we found in this study, that Scr3 is also secreted into the culture medium but in a form of extracellular microvesicles named exosomes, which are derived from ILVs (intraluminal vesicles) of MVBs (multivesicular bodies) [31–33]. Contrary to previous reports of mitochondrial localization of Scr3, we observed localization of Scr3 to other endomembrane systems including endosomes. Efficiency of Scr3 secretion was found to depend on palmitoylation of the Scr3 protein. Moreover, the secreted Scr3 protein was taken up by HeLa cells that were used as recipient cells, suggesting that the Scr3 protein is transferred from cells to cells in a paracrine manner.

MATERIALS AND METHODS

Antibodies and reagents

Rabbit pAbs (polyclonal antibodies) against mitochondrial marker protein TOM20 (sc-11415) and endosomal marker protein Rab5B (sc-598) and mouse mAb (monoclonal antibody) of anti-GFP (green fluorescent protein) (clone B2) were purchased from Santa Cruz Biotechnology. Mouse mAb of anti-GAPDH (glyceraldehyde-3-phosphate dehydrogenase, clone 6C5) was obtained from Chemicon. Anti-α-tubulin pAb (ab18251) was obtained from Abcam. Preparation of rabbit pAb against human ALG-2 was described previously [34]. Rabbit anti-mouse Alix (ALG-2-interacting protein X) pAb was also purchased from Covalab (CVL-PAB0204). Monoclonal antibodies against human Scr3 were obtained by immunizing mice with purified MBP (maltose-binding protein)-fused full-length Scr3, and hybridoma cells were screened by GST (glutathione transferase)-fused full-length Scr3 essentially as described previously [35]. IgG was affinity-purified with Protein G–Sepharose (see the Supplementary Materials and methods section at http://www.bioscirep.org/bsr/033/bsr033e026add.htm). 2-BP (2-bromopalmitate), HPβCD (hydroxypropyl-β-cyclodextrin) and GW4869 were purchased from Sigma–Aldrich. Trypsin was from Wako Pure Chemical Industries.

Plasmid construction

To construct an expression plasmid of Scr3 fused with GFP at its C-terminus (pScr3-GFP), an Scr3-encoding cDNA fragment of about 0.9 kb was amplified by PCR using specific primers listed in Supplementary Table S1 (at http://www.bioscirep.org/bsr/033/bsr033e026add.htm) and inserted at the XhoI/EcoRI sites of pEGFP (p-enhanced green fluorescent protein)-N1 using an In-Fusion HD cloning kit from Takara. Construction of expression plasmids for untagged human Scr3 (pIRESneo/Scr3) and GFP-fused WT (wild-type) and deletion mutants in the regions corresponding to the ABS (ALG-2-binding site) in the N-terminal Pro-rich region (pGFP-Scr3ΔABS1, pGFP-Scr3ΔABS2 and pGFP-Scr3ΔABS1/2) was described previously (renamed Scr3 in place of PLSCR3 for convenience) [24]. Deletion mutants of either the N-terminal or C-terminal domain were constructed by ligating either the EcoRI/BamHI or EcoRI fragment of pIRES1neo/Scr3 into the EcoRI/BamHI site of pEGFP-C2 or into the EcoRI site of pEGFP-C1, and the resultant plasmids are designated pGFP-Scr3ΔN and pGFP-Scr3ΔC, respectively. Expression plasmids for GFP–VPS4B^{E235Q} and GFP–Rab5A^{Q79L} were described previously [36,37]. Amino acid substitution mutations of cysteine residues with alanine residues at palmitoylation sites in Scr3 were performed by two sequential PCR methods. First, pIRES1neo/Scr3_3CA expressing Scr3 with three Cys mutations (Scr3_3CA, Cys at 162, 163 and 165 with Ala) was obtained by the overlap PCR method using pIRES1neo/Scr3 as a template and overlapped primers including the mutagenesis sites (Supplementary Table S1). Next, pIRES1neo/Scr3_4CA expressing Scr3 with four Cys mutations (Scr3_4CA, Cys at 160, 162, 163 and 165 with Ala) was obtained with a QuikChange Site-Directed Mutagenesis kit using pIRES1neo/Scr3_3CA as a template and specific oligonucleotide primers (Supplementary Table S1). The mutations were confirmed by DNA sequencing.

Cell culture and DNA transfection

HEK-293 cells and HeLa SS4 cells (subcloned HeLa cells, see [34]) were cultured in DMEM (Dulbecco's modified Eagle's medium) (Nissui) supplemented with 4 mM glutamine, 5 or 10 % FBS (fetal bovine serum), 100 units/ml penicillin and 100 μg/ml streptomycin at 37 °C under humidified air containing 5 % CO_2. At 1 day after the cells had been seeded, the cells were transfected with the expression plasmid DNAs by the conventional calcium phosphate precipitation method for HEK-293 cells or by using FuGENE 6 (Roche Applied Science) for HeLa cells. A cell line of ALG-2-knockdown and Scr3-expressing cells (HEK-293/Scr3/ALG-2_{KD}) was established by transfecting HEK-293/ALG-2_{KD} cells [38] with pIRES1neo/Scr3 as described previously (24).

Preparation of exosomal fractions and sucrose density gradient centrifugation

A cell line of HEK-293 cells stably expressing Scr3 (designated HEK-293/Scr3) was previously established by transfection of HEK-293 cells with pIRES1neo/Scr3 followed by screening of G418-resistant cells [24]. The cell culture medium was centrifuged at 10000 ***g*** for 15 min at 4 °C to remove cells and debris. The obtained supernatant was centrifuged at 100000 ***g*** (Beckman rotor TLA100.2, 46000 rev./min) for 60 min at 4 °C, and the pellet (crude exosomal fraction) was solubilized in SDS/PAGE sample buffer for analysis by WB (Western blotting). For sucrose density gradient centrifugation analysis, the 100000 ***g*** pellet was resuspended in 0.5 ml of 2.0 M sucrose in PBS (137 mM NaCl, 2.7 mM KCl, 8 mM Na_2HPO_4, 1.5 mM KH_2PO_4, pH 7.3) and then transferred to a 2-ml centrifuge tube and sequentially layered with lower concentrations of sucrose in PBS (0.5 ml of 1.5 M sucrose, 0.3 ml of 1.0 M sucrose, 0.3 ml of 0.63 M sucrose and 0.4 ml of 0.15 M sucrose). After centrifugation at 113000 ***g*** (Beckman TLS55 rotor, 40000 rev./min) for 18 h at 4 °C, fractions were collected from top to bottom of the 2-ml centrifuge tube with an automatic density gradient fraction collector (Advantec model CHD255AA). Density of each fraction was measured with a refractometer (IATC-1E for 0–32 % Brix, AS ONE and MASTER-2T for 28-62 % Brix, ATAGO).

Western blotting

For TCL (total cell lysate) preparation, cells were lysed with buffer H (10 mM HEPES-KOH, pH 7.4, 142.5 mM KCl, 1.5 mM $MgCl_2$, 0.1 mM pefabloc, 3 μg/ml leupeptin, 1 μM E-64, 1 μM pepstatin) containing 0.2 % NP-40 (Nonidet P40). Protein samples were resolved by SDS/PAGE, transferred to PVDF membranes (Immobilon-P, Millipore), and probed first with specific primary antibodies and next with HRP (horseradish peroxidase)-conjugated secondary antibodies essentially as described previously [24]. Chemiluminescent signals were detected with a LAS-3000mini lumino-image analyser (Fujifilm) using Super Signal West Pico Chemiluminescent Substrate (Thermo Fisher Scientific Inc). Densities of signals were measured with Multi Gauge Ver3.0 (Fujifilm).

Immunofluorescence microscopic analysis

One day after HeLa cells had been seeded on to 18×18 mm/mm coverglasses in 3-cm diameter dishes, they were transfected with 200 ng of the respective expression plasmid DNA. After 24 h, cells were fixed in 4 % PFA (paraformaldehyde)/PBS at 4 °C for 60 min, washed three times with 15 mM glycine/PBS, and permeabilized for 5 min in 0.1 % Triton X-100/PBS. After blocking with 0.1 % gelatin/PBS for 30 min, the cells were processed for immunocytochemistry essentially as described previously [39]. The fluorescence signals of GFP, TO-PRO-3 (DNA staining, Invitrogen/Molecular Probes) or fluorescent dye-labelled secondary antibodies, each specified in the Figure legends, were analysed with a confocal laser-scanning microscope, LSM5 PASCAL equipped with a ×63 oil-immersion objective (Plan-Apochromat ×63/1.40 Oil, Car Zeiss).

RESULTS

Secretion of Scr3 into culture medium

We previously established a cell line of HEK-293/Scr3 (Scr3-expressing HEK-293 cells) to analyse interactions between Scr3 and ALG-2 [24]. During the course of biochemical analyses using this cell line, we coincidentally found that Scr3 was released into the culture medium, as indicated by strong immunoreactive signals of anti-Scr3 mAb using the 10000 ***g*** supernatant of CM (conditioned medium; Culture sup) as a sample for Western blot analysis (Figure 1A, top panel). While intensities of signals for ALG-2 and GAPDH in HEK-293/Scr3 cells were similar to that of Scr3 in the TCL, signals were only faintly detected for ALG-2 and not detected for GAPDH in the culture supernatant under the condition used (middle and bottom panels), suggesting that release of Scr3 into the culture medium was not due to mere rupture of cell membranes. Interestingly, release of Scr3 was significantly reduced when we analysed a newly established cell line, designated HEK-293/Scr3/ALG-2_{KD}, in which expression of ALG-2 was constitutively suppressed by the RNA interference method.

Since Scr3 does not possess a signal sequence for secretion at its N-terminus, Scr3 should be secreted to the culture medium not by the classical ER–Golgi–plasma membrane pathway but by an unconventional secretory pathway either in soluble form or associated with or enclosed in membranous microvesicles [40]. To know the nature of unconventional secretion, we performed stepwise differential centrifugations of CM of HEK-293/Scr3 cells and analysed the distribution of Scr3 by WB. As shown in Figure 1(B), Scr3 was detected in the 1000 ***g*** (S_1) and 10000 ***g*** (S_2) supernatants with immunoreactive signal intensities similar to that of the CM. Scr3 was detected in the 100000 ***g*** pellets (P_3) but not in the 100000 ***g*** supernatant (S_3), suggesting secretion of Scr3 in the form of extracellular microvesicles. Some intracellular proteins are known to be secreted to culture medium as a form enclosed in exosomes. We investigated effects of ALG-2 knockdown on the efficiency of secretion of known exosome marker

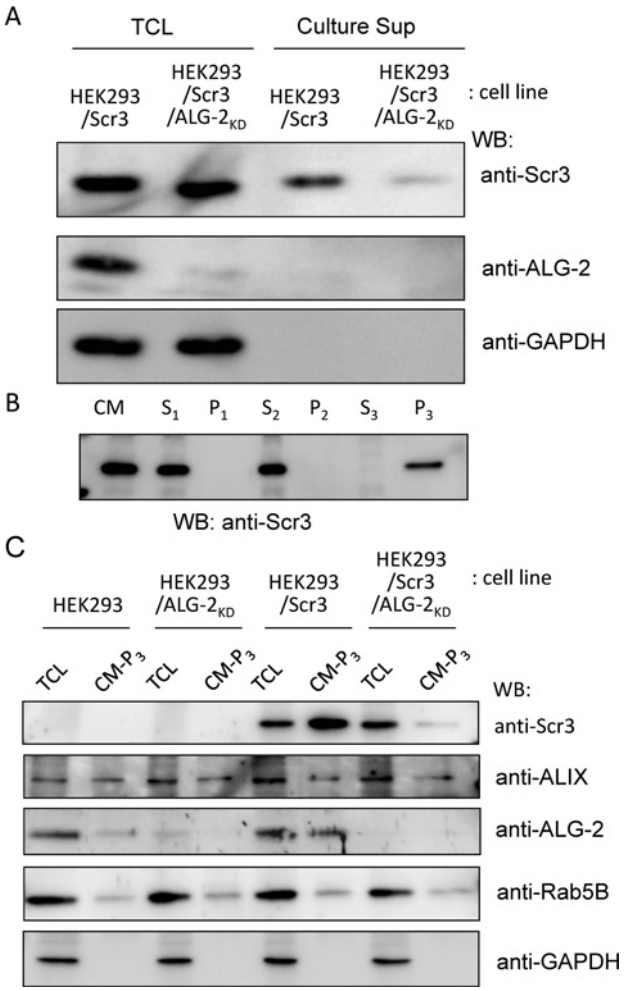

Figure 1 Secretion of Scr3 into culture medium

(**A**) HEK-293/Scr3 cells and Scr3-expressing ALG-2 knockdown HEK-293 cells (HEK-293/Scr3/ALG-2_{KD}) were cultured for 2 days, and each CM was centrifuged at 10 000 ***g*** for 15 min. The obtained culture supernatant (Culture Sup) and TCL were subjected to WB using anti-Scr3 mAb (top panel), anti-ALG-2 pAb (middle panel) and anti-GAPDH mAb (bottom panel). (**B**) CM of HEK-293/Scr3 cells was fractionated by sequential centrifugations at different gravities, and the supernatants and pellets were analysed for Scr3 by WB. S_1, supernatant of 1000 ***g***, 10 min; P_1, pellets of 1000 ***g***, 10 min; S_2, supernatant of centrifugation of S_1 at 10 000 ***g***, 15 min; P_2, pellets of centrifugation of S_1 at 10 000 ***g***, 15 min; S_3, supernatant of centrifugation of S_2 at 100 000 ***g***, 60 min; P_3, pellets of centrifugation of S_2 at 100 000 ***g***, 60 min. (**C**) TCL and pellets of centrifugation of S_2 at 100 000 ***g*** for 60 min of each CM-P_3 from HEK-293, HEK-293/ALG-2_{KD}, HEK-293/Scr3 and HEK-293/Scr3/ALG-2_{KD} cells were analysed for Scr3, Alix, ALG-2, Rab5B and GAPDH by WB using specific antibodies. Representative data obtained from three (**A**) and two (**B**, **C**) independent experiments are shown.

proteins such as Alix and Rab5B. As shown in Figure 1(C), Alix and Rab5B were detected in similar amounts in the crude exosomal fractions (CM-P_3, P_3 fraction of CM S_2) from all cell lines examined (HEK-293, HEK-293/ALG-2_{KD}, HEK-293/Scr3 and HEK-293/Scr3/ALG-2_{KD}), indicating that ALG-2 is not involved in exosome secretion in general. Secretion of ALG-2 was promoted by expression of Scr3.

Since expression of endogenous Scr3 was barely detectable in HEK-293 cells, we searched for human cell lines that express Scr3 and found that secretion of endogenous Scr3 was also observed when cells of T-24, a human bladder cancer cell line, were analysed (Supplementary Figure S2 at http://www.bioscirep.org/bsr/033/bsr033e026add.htm). However, the amount of Scr3 secreted from T-24 cells was estimated to be about 30-fold smaller than that from HEK-293/Scr3 cells by densitometric analyses of Western blot signals (percentages of analysed TCL and CM used for WB that give comparable signal intensity: 0.41 and 0.33 % for HEK-293/Scr3, 0.25 and 10 % for T-24, respectively), we selected the HEK-293/Scr3 cell line for further analyses of Scr3 secretion.

Presence of Scr3 inside the exosomes

Three types of major extracellular vesicles known as exosomes, shedding vesicles and apoptotic vesicles are generated by different mechanisms and can be distinguished by sizes, shapes and densities [31–33]. We performed sucrose density gradient centrifugation analysis of CM-P_3 (100 000 ***g*** pellet obtained from 10 000 ***g*** supernatant of CM) of HEK-293/Scr3 cells. As shown in Figure 2A, Scr3 was detected in fractions with the main peak at Nos. 6–7 having sucrose density of approx. 1.10 g/ml (Figure 2B), which agrees with the reported criteria of exosomes (density of 1.10–1.12 g/ml in flotation density). These fractions included Alix, ALG-2 and Rab5B, an endosomal marker. To determine whether Scr3 is secreted within membranous microvesicles or bound to the outer leaflets of membranes facing the culture medium, aliquots of exosome fractions after sucrose density gradient centrifugation were treated with trypsin. As shown in Figure 2(C), Scr3 was proteolysed by trypsin in the presence of 1 % Triton X-100 but not in the absence of the non-ionic detergent, indicating location of Scr3 inside the membranous vesicles.

Requirement of N-terminal region in Scr3 for secretion

To determine whether the ABSs in Scr3 are important for extracellular secretion of Scr3, we performed transient expression assays by transfection of HEK-293 cells with expression plasmids of various GFP-fused Scr3 mutants (see schematic representations in Figure 3A). First, effects of GFP-fusion and position of fusion to Scr3 were investigated. The amounts of secreted Scr3 estimated by WB of the exosomal fractions (100 000 ***g*** pellets obtained from 10 000 ***g*** supernatant of CM) were not significantly different among the N-terminal and C-terminal GFP-fused Scr3 (GFP–Scr3 against Scr3–GFP) and untagged Scr3 (Figure 3B, middle panel). Untagged GFP was not detected in the exosomal fraction. Next, expression plasmids of GFP–Scr3 with deletion in each or both of ΔABS1 and/or ΔABS2, the entire N-terminal Pro-rich region (ΔN) or the Scr conserved domain (ΔC) were used for transfection. Western blot signals

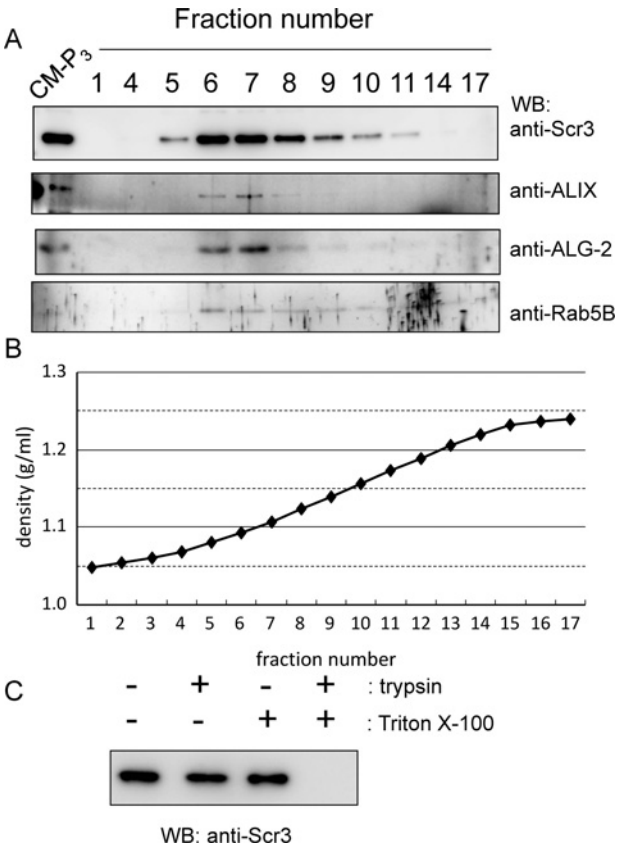

Figure 2 Scr3 in secreted exosomes

(**A**) and (**B**), 100 000 ***g*** pellet fraction of CM from HEK-293/Scr3 cells (CM-P_3) was resuspended in 2.0 M sucrose in PBS and layered step–wise with a sucrose cushion (1.5, 1.0, 0.5 and 0.25 M) as described in the Materials and methods section. The gradient was spun at 113 000 ***g*** for 18 h and fractions were collected from the top of the gradient. Each fraction was subjected to WB with antibodies against Scr3, Alix, ALG-2 and Rab5B (**A**) and to sucrose density measurement (**B**). (**C**) Aliquots of exosome fractions obtained by the sucrose density gradient centrifugation were used for a protease resistance assay by incubation with or without 0.1 mg/ml trypsin and 1% Triton X-100 for 20 min. Each sample was subjected to WB using anti-Scr3 antibody. Representative data obtained from three independent experiments are shown.

with anti-GFP mAb in the exosome fractions were not detected or only barely detected for control unfused GFP (ctrl) and GFP–ScrΔN but were detected for other deletion mutants and WT GFP–Scr3 (Figure 3C, top panel). However, relative efficiency of secretion was different among the mutants when comparing the amounts of Scr3 between the TCLs and exosomes. Although the amounts of GFP–Scr3ΔABS1 and GFP–Scr3ΔN were smaller than those in other constructs in TCLs, signals were detected for GFP–Scr3ΔABS1 but not for GFP–Scr3ΔN in the exosomal fractions. In contrast with the greater amount of GFP–Scr3ΔABS2 than GFP–Scr3ΔABS1 in TCLs, the amount of secreted GFP–Scr3ΔABS2 was equal to or smaller than that of GFP–Scr3ΔABS1. ABSs may affect stability of expressed proteins. Among the GFP-fused Scr3 proteins, immuno-reactive signals of anti-Scr3 mAb were not detected for the deletion mutants of ΔABS1, ΔABS1/2 and ΔN, indicating that an epitope for this antibody is located within ABS1 in the N-terminal Pro-rich region (Figure 3C, middle panel). The amounts of Alix in the exosomes were not influenced by differences in transfected DNAs (Figure 3C, bottom panel). Faster migrating bands in TCLs (indicated by an open arrowhead) may represent degradation products of Alix.

Effects of palmitoylation inhibition on secretion and subcellular localization

Murine Scr3 has been identified as a palmitoylated protein by LC–MS/MS (liquid chromatography–tandem MS) proteomic profiling of S-acylated macrophage proteins, and the palmitoylation site was determined (159-CGCSCCPC-166; corresponding to 158–165 in human Scr3) [41]. To investigate whether palmitoylation of Scr3 is involved in secretion, first we treated HEK-293/Scr3 cells with 2-BP, a palmitoylation inhibitor. As shown in Figure 4(A), while secretion of the exosomal marker protein Alix was not affected by 2-BP, secretion of Scr3 was significantly suppressed in comparison with the treatment with a vehicle (0.5% ethanol) as a negative control (ctrl). Immunofluorescence microscopic analysis was performed to determine the effect of 2-BP on subcellular localization of Scr3 in HEK-293/Scr3 cells (Figure 4B). Specific immunofluorescence signals of Scr3 were barely detectable in the parental HEK-293 cells but were clearly observed in HEK-293/Scr3 cells in the cytoplasm in the absence of 2-BP. In the presence of 2-BP, the fluorescence signals were largely found in the nucleus that was visualized with DNA staining with TO-PRO-3. Scr3 and TOM20, a mitochondrial marker, did not show colocalization in the presence or absence of 2-BP. A similar cytoplasmic punctate pattern of Scr3 and non-colocalization with TOM20 were observed in HeLa cells that expressed Scr3 transiently by the DNA transfection experiment (Supplementary Figure S3e at http://www.bioscirep.org/bsr/033/bsr033e026add.htm).

It remained to be clarified whether suppression of exosomal secretion of Scr3 by 2-BP was due to inhibition of palmitoylation of either Scr3 itself or other palmitoylated proteins. To address this question, as shown in Figure 5(A), we constructed expression plasmids of untagged Scr3 mutants in which either three or four cysteine residues were substituted with alanine (Scr3_3CA or Scr3_4CA) in the corresponding sequence of the previously determined palmitoylation site of murine Scr3 [41]. As shown in Figure 5(B), the WT Scr3 protein was consistently detected by WB in the exosomal fraction, but the amount of secreted Scr3_3CA protein markedly decreased, and secretion of the Scr3_4CA protein was barely detectable as in the case of the negative control (ctrl) in which an empty vector was used for transfection. Conversely, the amounts of palmitoylation-defective mutant Scr3 proteins increased in the TCLs compared with the WT Scr3 protein. In agreement with previous reports on murine palmitoylation-defective mutants of Scr1 and Scr3 [3,41], fluorescence microscopic analyses showed localization of these mutants in the nucleus (results not shown).

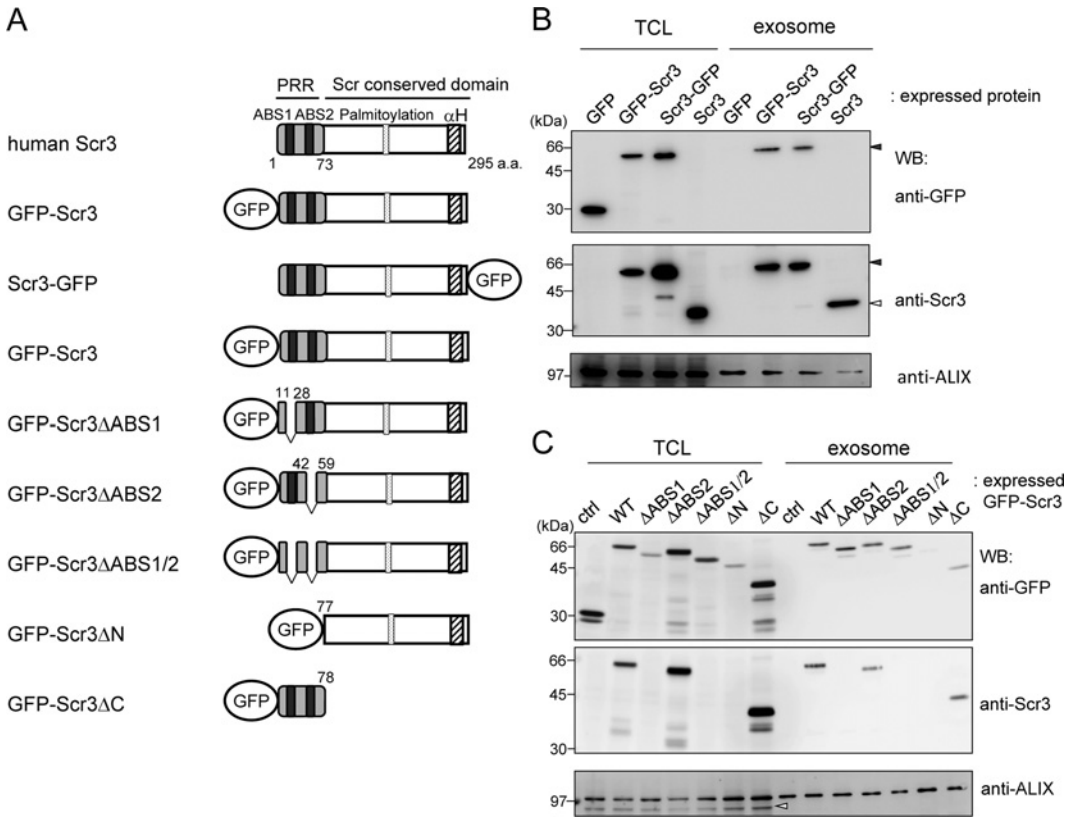

Figure 3 **Requirement of N-terminal region in Scr3 for exosomal secretion**

(**A**) The various GFP-fused Scr3 expression constructs used in this study are schematically represented. The N-terminal PRR (pro-rich region) including ABS1 and ABS2, palmitoylation motif and C-terminal α-helix (αH) are indicated. Full-length or mutants of deletion in ABS1 (ΔABS1), ABS2 (ΔABS2), both ABS1 and ABS2 (ΔABS1/2), N-terminal region (ΔN) and Scr conserved domain (ΔC) were prepared as fusion proteins with GFP. The numbers denote the amino acid (a.a.) positions in each construct. (**B**) HEK-293 cells were transfected with each plasmid that expresses GFP as a negative control or GFP fused with Scr3 at either N-terminus (GFP–Scr3) or C-terminus (Scr3-GFP). TCL and 100 000 ***g*** pellet fraction (exosome) from each CM of transfected HEK-293 cells were subjected to WB with antibodies against GFP, Scr3 and Alix. (**C**) HEK-293 cells were transfected with plasmids expressing GFP (ctrl) or GFP-fused with either WT or various deletion mutants of Scr3, and expressed proteins were similarly analysed by WB as shown in (**B**). Open arrowhead indicates a non-specific or degraded band of Alix in TCL (bottom panel). Representative data obtained from three independent experiments are shown.

Effects of disturbance of endosomal membrane traffic on secretion of Scr3

Exosomes are thought to be derived from MVB ILVs that are released into extracellular space after fusion of MVBs with plasma membranes [31,32]. ILVs are generated by inward budding of the endosomal membrane into the lumen, the process of which is catalysed by the ESCRT (endosomal sorting complex required for transport) machinery. To investigate whether secretion of Scr3 passes through the endosome–MVB pathway, we coexpressed Scr3 in HEK-293 cells with either one of two representative factors affecting endosomal membrane trafficking and estimated secretion efficiency: (i) a dominant-negative form of GFP-fused ATPase-defective AAA (ATPase associated with various cellular activities)-type ATPase VPS4B (VPS4B^{E235Q}, glutamate replaced with glutamine at position 235) that causes stacking of ESCRT-III subunits on the endosomal membranes by aborting disassembly of the subunits, and (ii) GFP-fused GTP-locked mutant of Rab5A (Rab5A^{Q79L}, glutamine replaced with leucine at position 79) that causes enlargement of endosomes. As shown in Figure 6(A), the amount of secreted Scr3 in the exosomal fraction was significantly reduced by overexpression of GFP–VPS4B^{E235Q}. Considering the relative ratio of the amounts of Scr3 remaining in TCLs and secreted as exosomes, calculated secretion efficiency was decreased to 3 % by overexpression of GFP–VPS4B^{E235Q} and to 65 % by overexpression of GFP–Rab5A^{Q79L} in comparison with the control GFP expression vector (ctrl, 100 %) (Figure 6B). Increase in the amounts of Scr3 in TCLs of the mutant-expressing cells in comparison with that in the case of expression of GFP (ctrl) may be due to suppression of degradation in lysosomes. Secretion of endogenous Alix was not significantly affected by overexpression of GFP–VPS4B^{E235Q} (Figure 6A, bottom panel). It is likely that only a small proportion of HEK-293 cells were affected by overexpressed GFP–VPS4B^{E235Q} due to lower transfection efficiency under the condition used. Indeed, when HEK-293/Scr3

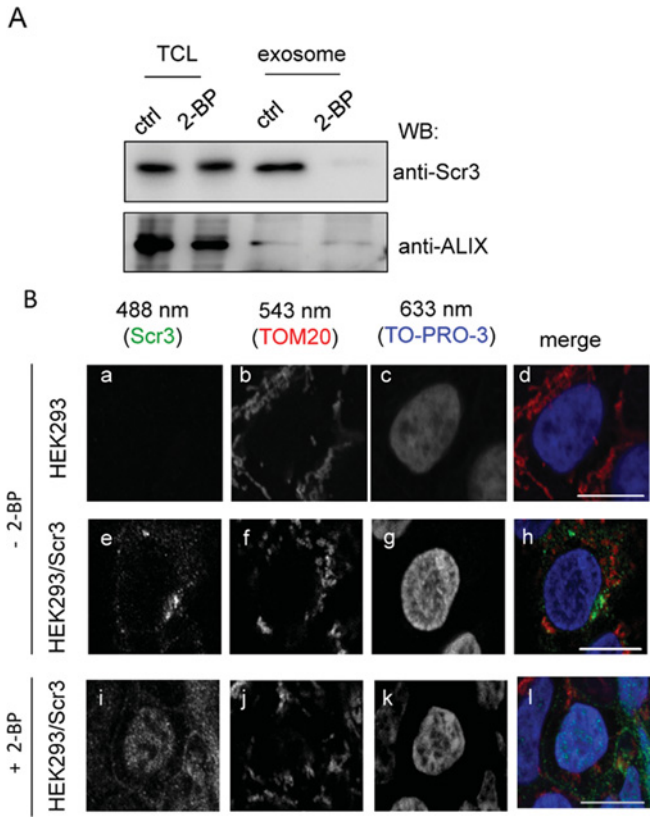

Figure 4 Effects of palmitoylation inhibitor on secretion and intracellular localization of Scr3

(**A**) After HEK-293/Scr3 cells had been cultured for 24 h in the presence of 50 μM 2-BP or a vehicle (0.5% ethanol) as a control (ctrl), TCL and 100 000 ***g*** pellet fraction (exosome) of each CM were subjected to WB with antibodies against Scr3 and Alix. (**B**) Either HEK-293 or HEK-293/Scr3 cells were cultured on poly-L-lysine-coated coverglasses in the presence or absence of 2-BP. After fixation, cells were permeabilized with 0.1% Triton X-100 for 5 min and then immuno-stained with anti-Scr3 mAb and anti-TOM20 pAb and stained with TO-PRO-3 for chromosomal DNA. Fluorescent signals of secondary antibodies of Alexa Fluor 488-conjugated anti-mouse IgG (Scr3: a, e, i; excitation at 488 nm) and Cy3-labelled anti-rabbit IgG (TOM20: b, f, j; excitation at 543 nm), and the signals of TO-PRO-3 (c, g, k; excitation at 633 nm) were analysed with a confocal laser-scanning microscope and are represented in black and white. Merged images are shown in colour (d, h, l) for Scr3 (green), TOM20 (red) and TO-PRO-3 (blue). Bars, 10 μm. Representative data obtained from three (**A**) and two (**B**) independent experiments are shown.

cells were transfected with the plasmid for GFP–VPS4B^{E235Q}, suppression of Scr3 secretion was only partially observed (results not shown).

In separate experiments using HEK-293/Scr3 cells, we investigated the effects of expression of these mutant proteins on subcellular distribution of Scr3 by immunofluorescence microscopy. As shown in Figure 6(C), punctate immunofluorescence signals were observed for Scr3 [white and red signals in panels (b) and (d), respectively] in GFP-expressing cells. On the other hand, punctate signals of Scr3 became larger [white and red signals in panels (f) and (h), respectively] and partly merged or juxtaposed with signals of GFP–VPS4B^{E235Q} [white and green signals in panels (e) and (h), respectively] in the perinuclear region [chromosomal DNA stained with TO-PRO-3, white and blue signals in panels (g) and (h), respectively]. Punctate signals of Scr3 were found at abnormally enlarged endosomes represented by GFP–Rab5A^{Q79L} [white and green signals in panels (i) and (l), respectively]. While colocalization of GFP–Rab5A^{Q79L} and Scr3 was clearly observed in HeLa cells by co-transfection experiments, colocalization of GFP–VPS4B^{E235Q} and Scr3 was limited (Supplementary Figure S4 at http://www.bioscirep.org/bsr/033/bsr033e026add.htm).

Effects of ceramide synthesis inhibition and cholesterol depletion on Scr3 secretion

Ceramide, a breakdown product of sphingomyelin, is involved in biogenesis of MVB, and inhibition of nSMase (neutral sphingomyelinase) by GW4869 was reported to suppress exosome release [42]. We investigated the time course of Scr3 secretion by measuring the amounts of Scr3 in the culture supernatant by Western blot analysis using an aliquot of medium taken at a 3-h interval after changing with a fresh medium containing 2-BP, HPβCD, a membrane cholesterol depletion reagent) or

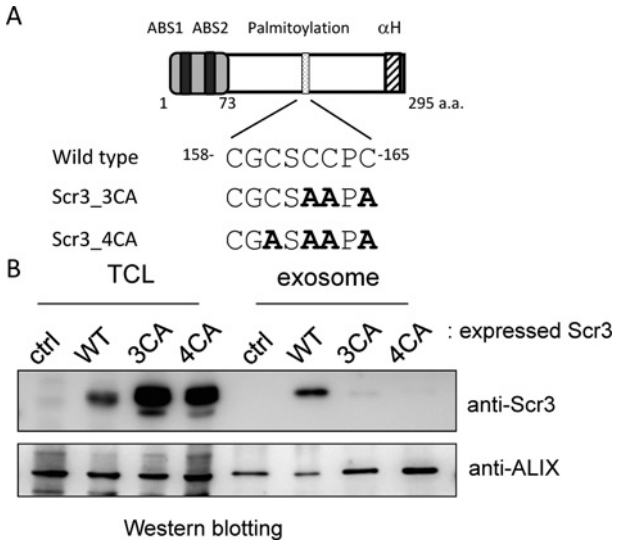

Figure 5 Effects of palmitoylation site mutation on secretion of Scr3

(**A**) Amino acid sequence of the palmitoylation site in Scr3 is displayed. Three and four cysteine residues at the positions indicated by bold face were substituted with alanine residues to create mutants designated as Scr3_3CA and Scr3_4CA, respectively. (**B**) HEK-293 cells were transfected with plasmids that express untagged WT Scr3, Scr3_3CA (3CA) or Scr3_4CA (4CA) or with an empty vector (pIRES1neo) used as a control (ctrl). TCL and 100 000 ***g*** pellet fraction (exosome) of each CM of transfected HEK-293 cells were subjected to WB using anti-Scr3 mAb and anti-Alix pAb. Representative data obtained from three independent experiments are shown.

GW4869 (Figure 7A). Immuno-reactive signals became unambiguously detectable 6 h after changing with the medium containing 0.16 % DMSO as a control (ctrl, top panel), and the amounts of secreted Scr3 gradually increased until 24 h. While addition of 2-BP (second row panel) and GW4869 (bottom panel) significantly reduced the amounts of secreted Scr3, HPβCD (third row panel) had little effect. As shown in Figure 7(B), top panel, similar inhibitory effects were observed when Scr3 in exosomal fractions (100 000 ***g*** pellets) were analysed. Importantly, 2-BP had no obvious adverse effects on secretion of non-palmitoylated proteins such as Alix (middle panel) and ALG-2 (bottom panel), but secretion of these proteins was also inhibited by GW4869. On the other hand, HPβCD slightly enhanced exosomal secretion of Scr3 as well as Alix and ALG-2. The reason for the discrepancy in effects of HPβCD on efficiency of Scr3 secretion between assay methods (no effect in culture supernatant compared with enhancement in exosome) is not clear. Cholesterol depletion may stabilize exosomes and increase the recovery efficiency from the culture supernatant. Alternatively, cholesterol depletion may enhance exosomal secretion of Scr3, but suppress its non-exosomal secretion.

Uptake of secreted Scr3 by recipient cultured cells

Exosomes are known to play roles in intercellular communications by carrying cargoes (such as proteins, mRNA and miRNA) that are transferred from exosome-releasing cells to recipient cells [31,32,43]. To investigate whether secreted Scr3 is also transferred from cells to cells, HeLa cells were cultured in a fresh medium mixed with an equal part of the culture supernatant derived from HEK-293/Scr3 cells for 2 days, immunostained with anti-Scr3 mAb, and analysed by fluorescence microscopy. As shown in Figure 8, immunoreactive fluorescent signals were observed in a punctate pattern in the perinuclear region of HeLa cells using the culture supernatant derived from HEK-293/Scr3 cells [panel (e)] but not that derived from HEK-293 cells [panel (a)].

DISCUSSION

Exosomes are extracellular microvesicles (50–100 nm in diameter) released from eukaryotic cells and play roles in intercellular communication by transferring not only proteins and lipids but also RNAs including mRNA and miRNA to recipient cells [31,32,43]. Exosomes derived from ILVs in the MVB are released into extracellular space after fusion of MVBs with plasma membranes [31,32], and they are distinguished from shedding vesicles (100–1000 nm in size) that are released directly from plasma membranes after outward budding on the membranes [33]. Proteomics of purified exosomes using LC–MS/MS have identified hundreds of intracellular and membrane proteins [44–46], and the number of identified proteins listed in ExoCarta (http://www.exocarta.org/) exceeds 1000 for mammalian exosomes (2557 for humans, 1259 for mice, 2127 for rats as of October 29, 2012). Scr1 (*PLSCR1*) and Scr3 (*PLSCR3*) were also documented by proteomics of exosomes prepared from urine [44] and a colon tumour cell line [47], respectively. Here we showed exosomal secretion of not only exogenously expressed Scr3 from HEK-293 cells (Figures 1 and 2) but also endogenous Scr3 from T-24 cells (Supplementary Figure S2). Merregaert et al. [30] reported that Scr1 was secreted by a lipid raft-dependent mechanism from HaCaT keratinocytes and deposited in the ECM by interacting with ECM1. In the present study, we demonstrated that secretory pathways are different for Scr1 and Scr3. While secretion of Scr1 was reported to be suppressed by a cholesterol depletion reagent but not by a palmitoylation inhibitor [30], effects of these reagents were opposite towards the secretion of Scr3: suppression by 2-BP (Figures 4A and 7) but not by HPβCD (Figure 7). Requirement of palmitoylation reaction for secretion is most likely due to the lipid modification of Scr3 itself as revealed by failure in secretion of the mutants with amino acid substitutions at the palmitoylation sites (Figure 5).

Trajkovic et al. [42] reported that proteolipid protein is secreted from Oli-neu cells as exosomes and proposed that exosome-secreting MVBs are distinguished from lysosome-destined MVBs based on requirements of factors for MVB biogenesis, i.e., while the former MVBs require sphingolipid ceramide but not ESCRTs, the latter MVBs require ESCRTs. Secretion of Scr3 was significantly suppressed by GW4869, an inhibitor of ceramide synthesis (Figure 7). However, co-expression of a

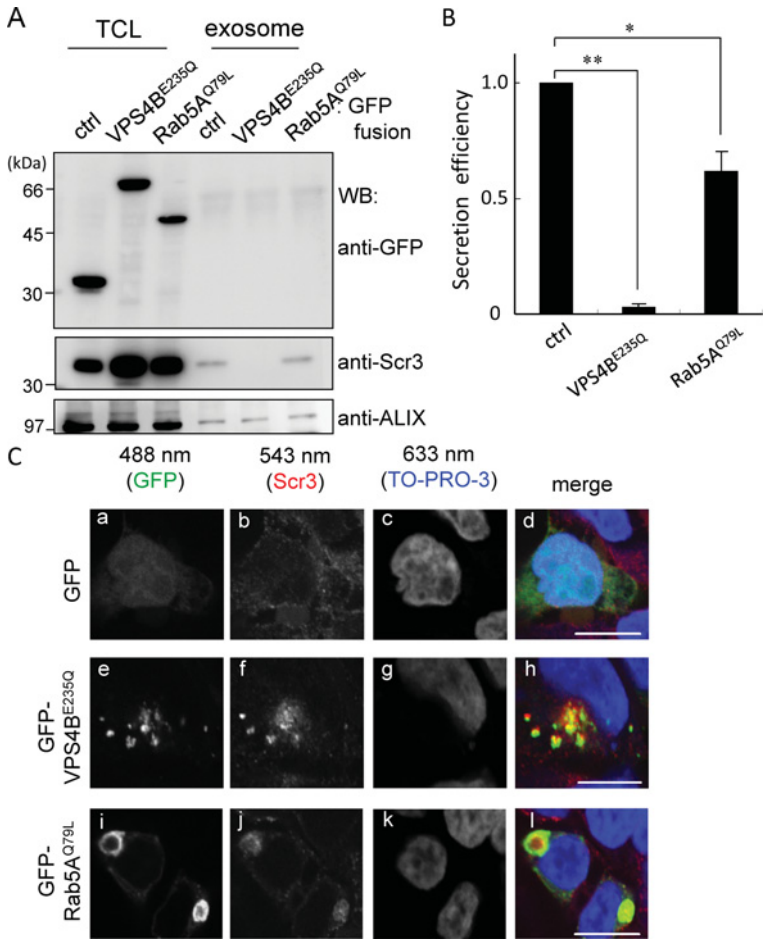

Figure 6 Effects of disturbance of endosomal membrane traffic on secretion of Scr3

(**A**) HEK-293 cells were co-transfected with pIRES1neo/Scr3 and expression plasmids for GFP–VPS4B^{E235Q}, GFP–Rab5^{Q79L} or GFP as a control (ctrl). TCL and 100 000 ***g*** pellet fraction (exosome) of the CM from the transfected HEK-293 cells were subjected to WB with antibodies against GFP, Scr3 and Alix. (**B**) Intensities of WB signals of Scr3 in TCLs and exosomal fractions were quantified and relative secretion efficiencies were calculated by using the value of 1.0 for the control (ctrl). Three independent transfection experiments were performed and calculated values were expressed as means $\pm$ S.E.M. ($n = 3$). Statistically significant differences of effects on Scr3 secretion were evaluated by Student's *t* test by comparing the secretion efficiency with the control GFP and GFP-fusion proteins ($*P < 0.05$; $**P < 0.01$). (**C**) HEK-293 cells cultured on poly-L-lysine-coated coverglasses were co-transfected with pIRES1neo/Scr3 and expression plasmids for GFP–VPS4B^{E235Q}, GFP–Rab5A^{Q79L} or GFP as a control. One day after transfection, the cells were processed for immunocytochemistry using anti-Scr3 mAb and Cy3-conjugated goat anti-mouse IgG. Nuclei were stained with TO-PRO-3. Fluorescence signals of GFP (excitation at 488 nm: a, e and i), Cy3 (excitation at 543 nm: b, f and j) and TO-PRO-3 (excitation at 633 nm: c, g, k) were analysed with a confocal laser scanning microscope and are represented in black and white. Merged images are shown in colour (d, h, l) for GFP (green), Scr3 (red) and TO-PRO-3 (blue). Bars, 10 μm. Representative data obtained from three independent experiments are shown.

dominant-negative form of VPS4B protein (GFP–VPS4B^{E235Q}) also significantly suppressed secretion of Scr3 from HEK-293 cells in transient transfection experiments (Figures 6A and 6B). Since VPS4B is an AAA ATPase involved in recycling of ESCRT-III subunits on endosomal membranes and the dominant-negative mutant impairs MVB biogenesis, it is likely that transport of Scr3 from endosomes to MVB depends on the ESCRT system. Secretion of syndecan-containing exosomes requires ceramide as well as the ESCRT machinery and Alix, which interacts with syntenin (adaptor of syndecan) as well as CHMP4s (subunits of ESCRT-III) [48]. Requirement of ESCRTs for exosomal secretion may depend on cargoes to be analysed, and ceramide dependency and ESCRT dependency are not mutually exclusive mechanisms. The suppressive effect of the constitutive active Rab5A mutant on exosomal secretion of Scr3 (Figures 6A and 6B) agrees with the results of previous studies on secretion of proteolipid protein and syndecan [42,48]. Overexpression of GFP–VPS4B^{E235Q} did not inhibit exosomal secretion of Alix (Figure 6A). Since Alix is involved in formation of MVE (multivesicular endosomes) by associating with the MVE-specific unconventional phospholipid

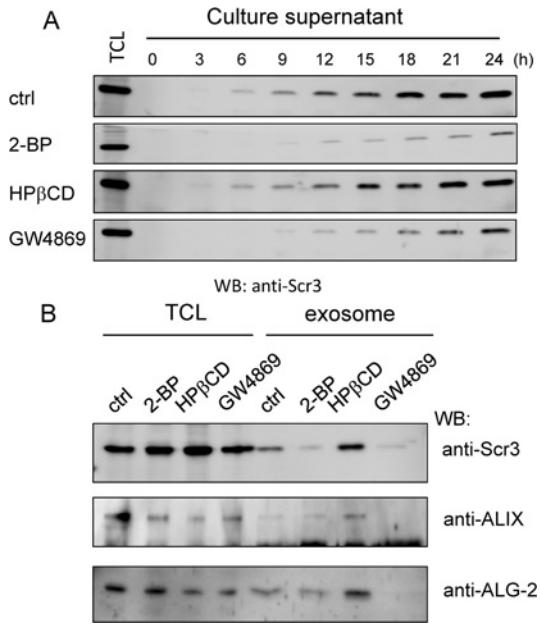

Figure 7 Effects of ceramide synthesis inhibition and cholesterol depletion on Scr3 secretion

(**A**) HEK-293/Scr3 cells were cultured in the presence of either 0.16% DMSO (ctrl), 50 μM 2-BP, HPβCD or 5 μM GW4869 (nSMase inhibitor) for up to 24 h. At the indicated time, each aliquot of the culture medium was centrifuged at 10 000 ***g*** to remove cell debris, and the culture supernatants were subjected to WB using anti-Scr3 mAb. (**B**) After HEK-293/Scr3 cells had been cultured for 24 h in the presence of reagents used in (**A**), TCL and 100 000 ***g*** pellet fraction (exosome) of each CM were subjected to WB with antibodies against Scr3, Alix and ALG-2. Representative data obtained from two (**A**) and three (**B**) independent experiments are shown.

2,2′-lysobisphosphatidic acid [49], there may exist multiple pathways for exosomal secretion of Alix, one of which is not regulated by ESCRTs.

Recently, ARRDC1 (arrestin domain-containing protein 1) ARMMs (ARRDC1-mediated microvesicles) have been shown to be formed at the plasma membrane and to have a size (~45 nm) similar to that of exosomes [50]. ARRDC1 has a PSAP motif and PPEY/PPSY motifs which recruit TSG101, a subunit of ESCRT-1, and NEDD4-like ubiquitin E3 ligase respectively. Release of the vesicles is affected by expression of the dominant-negative VPS4 mutant. This intrinsic cellular process called DPMB (direct plasma membrane budding) more resembles retrovirus release from host cells than MVB biogenesis at endosomes. Release of Scr3-containing exosomes may not be by DPMB based on the following observations: (i) Scr3 was found to be partially colocalized with GFP–VPS4B^{E235Q} in transfected cells by fluorescence microscopic analyses, and it colocalized well with endosomes enlarged by GFP–Rab5A^{Q79L} (Figure 6C), and (ii) secreted Scr3 in the culture medium was recovered in microvesicles that contained Rab5B, one of the exosome marker proteins known to be absent in DPMB vesicles (Figure 2A).

Although PLSCRs were initially predicted to be C-tail-anchored type II transmembrane proteins [2,17], the C-terminal hydrophobic α-helix regions of PLSCRs including Scr3 have been predicted by structural modelling to be buried within the core structure of the β barrel with 12 anti-parallel strands as in the case of TULPs ([25] and Supplementary Figure S1). In support of this model, fusion of a bulky GFP protein to Scr3 at the C-terminus, presumed to be inhibitory for membrane integration, did not influence the exosomal secretion of Scr3 in comparison with the N-terminal fusion (Figure 3B). Moreover, amino acid substitutions of palmitoylation sites, which are located in a large loop connecting β_5 and β_6 strands facing the exit side of the C-terminal α-helix passing through the barrel core (Supplementary Figure S5 at http://www.bioscirep.org/bsr/033/bsr033e026add.htm), caused translocation of the mutant Scr1 and Scr3 proteins from membranes to the nucleus [3,41], and nuclear translocation was also observed when HEK-293/Scr3 cells were treated with 2-BP (Figure 4). Although mitochondrial localization of Scr3 has been shown by subcellular fractionation, immunofluorescence microscopy and electron microscopy [18,21,51], the data presented in those reports did not indicate whether the majority of Scr3 localizes in mitochondria or whether only a small proportion of Scr3 localizes to this organelle. In our immunofluorescence microscopic analyses of HEK-293/Scr3 cells (Figure 4B) and HeLa cells transfected with Scr3-expressing plasmids (Supplementary Figure S3), the majority of immunofluorescent signals of Scr3 did not merge with fluorescent signals of mitochondrial markers. Colocalization of Scr3 with GFP–VPS4B^{E235Q} and GFP–Rab5A^{Q79L} suggests the existence of Scr3 in endosomal membranes (Figure 6C and Supplementary Figure S4).

While Scr1 and TULP1 are secreted and bind to the ECM1 and cell surface receptors in the extracellular space, respectively, most of the secreted Scr3 is recovered as exosomes in 100 000 ***g*** pellets by centrifugation (Figure 1B) and protected from protease attack (Figure 2C). Differences in secretory pathways for Scr1 and Scr3 may arise from the differences in subcellular localization (Scr1, plasma membranes against Scr3, endosomes). Both Scr1 and Scr3 have similar overall structures (48% amino acid identities), but the N-terminal Pro-rich regions are less conserved between them (Scr1, 18–97 against Scr3, 6–73: 30%). Since the Pro-rich region was necessary for exosomal secretion of Scr3 (Figure 3C), it may play an important role in the secretory pathway. ALG-2 associates with Scr3 but only weakly with Scr1 [24]. At first, we speculated that ALG-2 is involved in exosomal secretion of Scr3 after finding that an established cell line of ALG-2-deficient HEK-293/Scr3/ALG-2$_{KD}$ cells secretes a smaller amount of Scr3 proteins (Figure 1A). Knockdown of ALG-2 showed no adverse effects on exosomal secretion of Alix and Rab5B (Figure 1C). Deletion mutants of GFP–Scr3 in ABS1 and ABS2 had no or little effects on the amounts of secreted Scr3 (Figure 3C). Since transient knockdown of ALG-2 using siRNA (small interfering RNA) did not cause a decrease in the amount of secreted Scr3 (results not shown), HEK-293/Scr3/ALG-2$_{KD}$ might have adapted to poor Scr3 secretion during establishment of the cell line by unknown mechanisms. Increase in the amount of ALG-2 in exosomes by expressing Scr3 in HEK-293 cells (Figure 1C, HEK-293 compared with HEK-293/Scr3) and concomitantly

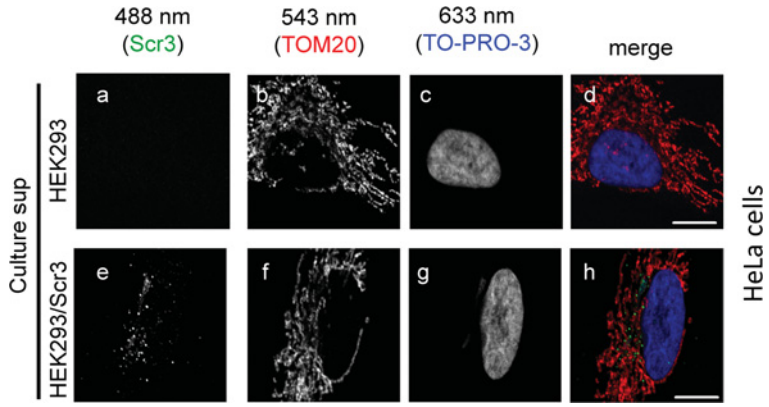

Figure 8 Uptake of secreted Scr3 by HeLa

CM of either HEK-293 cells or HEK-293/Scr3 cells that had been cultured for 48 h was centrifuged at 1000 ***g***, and the supernatant (Culture sup) was mixed 1:1 with the fresh medium and used to culture HeLa cells that had been seeded on coverglasses. After 48 h, cells were fixed and triple-stained with anti-Scr3 mAb (a, e), anti-TOM20 pAb (b, f) and TO-PRO-3 (c, g) and then analysed with a confocal laser-scanning microscope as described in the legend to Figure 4. Merged images are shown in (d) and (h) in colour. Bars, 10 μm. Representative data obtained from three independent experiments are shown.

enhanced exosomal secretion of both Scr3 and ALG-2 by HPβCD treatment (Figure 7B) suggest that Scr3 promotes secretion of its binding partner. Since secreted Scr3 can be taken up by HeLa cells, it may have a potential to function as a cell-to-cell communication molecule. Finding of the TULP superfamily member Scr3 as an exosomally secreted paracrine molecule would give us new insight into the roles of Scr3 in cells.

AUTHOR CONTRIBUTION

Tatsutoshi Inuzuka, Akira Inokawa and Cen Chen carried out the experiments. Kumiko Kizu and Hiroshi Narita prepared the monoclonal antibodies of Scr3. Tatsutoshi Inuzuka and Masatoshi Maki designed the study. Hideki Shibata advised on the experiments.

ACKNOWLEDGEMENTS

We thank Dr Bateman for providing us the PDB format file of the predicted model structure of Scr1 and Mr Takahashi for computer modelling of Scr3.

FUNDING

This work was supported by Grant-In-Aid for Scientific Research (B) and Research Fellowships from the Japan Society for the Promotion of Science (JSPS) to M. M. [project numbers 23380056 (to M.M.) and 22006388 (to T. I.)].

REFERENCES

1 Basse, F., Stout, J. G., Sims, P. J. and Wiedmer, T. (1996) Isolation of an erythrocyte membrane protein that mediates Ca^{2+}-dependent transbilayer movement of phospholipid. J. Biol. Chem. **271**, 17205–17210

2 Zhou, Q., Zhao, J., Stout, J. G., Luhm, R. A., Wiedmer, T. and Sims, P. J. (1997) Molecular cloning of human plasma membrane phospholipid scramblase. A protein mediating transbilayer movement of plasma membrane phospholipids. J. Biol. Chem. **272**, 18240–18244

3 Wiedmer, T., Zhao, J., Nanjundan, M. and Sims, P. J. (2003) Palmitoylation of phospholipid scramblase 1 controls its distribution between nucleus and plasma membrane. Biochemistry **42**, 1227–1233

4 Zhou, Q., Ben-Efraim, I., Bigcas, J. L., Junqueira, D., Wiedmer, T. and Sims, P. J. (2005) Phospholipid scramblase 1 binds to the promoter region of the inositol 1,4,5-triphosphate receptor type 1 gene to enhance its expression. J. Biol. Chem. **280**, 35062–35068

5 Chen, C. W., Sowden, M., Zhao, Q., Wiedmer, T. and Sims, P. J. (2011) Nuclear phospholipid scramblase 1 prolongs the mitotic expansion of granulocyte precursors during G-CSF-induced granulopoiesis. J. Leukoc. Biol. **90**, 221–233

6 Kusano, S. and Eizuru, Y. (2012) Human phospholipid scramblase 1 interacts with and regulates transactivation of HTLV-1 Tax. Virology **432**, 343–352

7 Zhou, Q., Zhao, J., Wiedmer, T. and Sims, P. J. (2002) Normal hemostasis but defective hematopoietic response to growth factors in mice deficient in phospholipid scramblase 1. Blood **99**, 4030–4038

8 Sun, J., Nanjundan, M., Pike, L. J., Wiedmer, T. and Sims, P. J. (2002) Plasma membrane phospholipid scramblase 1 is enriched in lipid rafts and interacts with the epidermal growth factor receptor. Biochemistry **41**, 6338–6345

9 Py, B., Basmaciogullari, S., Bouchet, J., Zarka, M., Moura, I. C., Benhamou, M., Monteiro, R. C., Hocini, H., Madrid, R. and Benichou, S. (2009) The phospholipid scramblases 1 and 4 are cellular receptors for the secretory leukocyte protease inhibitor and interact with CD4 at the plasma membrane. PLoS ONE **4**, e5006

10 Cusick, J. K., Mustian, A., Jacobs, A. T. and Reyland, M. E. (2012) Identification of PLSCR1 as a protein that interacts with RELT family members. Mol. Cell. Biochem. **362**, 55–63

11 Talukder, A. H., Bao, M., Kim, T. W., Facchinetti, V., Hanabuchi, S., Bover, L., Zal, T. and Liu, Y. J. (2012) Phospholipid Scramblase 1 regulates Toll-like receptor 9-mediated type I interferon production in plasmacytoid dendritic cells. Cell Res. **22**, 1129–1139

12 Amir-Moazami, O., Alexia, C., Charles, N., Launay, P., Monteiro, R. C. and Benhamou, M. (2008) Phospholipid scramblase 1 modulates a selected set of IgE receptor-mediated mast cell responses through LAT-dependent pathway. J. Biol. Chem. **283**, 25514–25523
13 Suzuki, J., Umeda, M., Sims, P. J. and Nagata, S. (2010) Calcium-dependent phospholipid scrambling by TMEM16F. Nature **468**, 834–838
14 Castoldi, E., Collins, P. W., Williamson, P. L. and Bevers, E. M. (2011) Compound heterozygosity for 2 novel TMEM16F mutations in a patient with Scott syndrome. Blood **117**, 4399–4400
15 Bevers, E. M. and Williamson, P. L. (2010) Phospholipid scramblase: an update. FEBS Lett. **584**, 2724–2730
16 Lhermusier, T., Chap, H. and Payrastre, B. (2011) Platelet membrane phospholipid asymmetry: from the characterization of a scramblase activity to the identification of an essential protein mutated in Scott syndrome. J Thromb. Haemost. **9**, 1883–1891
17 Wiedmer, T., Zhou, Q., Kwoh, D. Y. and Sims, P. J. (2000) Identification of three new members of the phospholipid scramblase gene family. Biochim. Biophys. Acta **1467**, 244–253
18 Liu, J., Dai, Q., Chen, J., Durrant, D., Freeman, A., Liu, T., Grossman, D. and Lee, R. M. (2003) Phospholipid scramblase 3 controls mitochondrial structure, function, and apoptotic response. Mol. Cancer Res. **1**, 892–902
19 Van, Q., Liu, J., Lu, B., Feingold, K. R., Shi, Y., Lee, R. M. and Hatch, G. M. (2007) Phospholipid scramblase-3 regulates cardiolipin de novo biosynthesis and its resynthesis in growing HeLa cells. Biochem. J. **401**, 103–109
20 Liu, J., Epand, R. F., Durrant, D., Grossman, D., Chi, N. W., Epand, R. M. and Lee, R. M. (2008) Role of phospholipid scramblase 3 in the regulation of tumor necrosis factor-α-induced apoptosis. Biochemistry **47**, 4518–4529
21 Ndebele, K., Gona, P., Jin, T. G., Benhaga, N., Chalah, A., Degli-Esposti, M. and Khosravi-Far, R. (2008) Tumor necrosis factor (TNF)-related apoptosis-inducing ligand (TRAIL) induced mitochondrial pathway to apoptosis and caspase activation is potentiated by phospholipid scramblase-3. Apoptosis **13**, 845–856
22 Wiedmer, T., Zhao, J., Li, L., Zhou, Q., Hevener, A., Olefsky, J. M., Curtiss, L. K. and Sims, P. J. (2004) Adiposity, dyslipidemia, and insulin resistance in mice with targeted deletion of phospholipid scramblase 3 (PLSCR3). Proc. Natl. Acad. Sci. U.S.A. **101**, 13296–13301
23 Maki, M., Kitaura, Y., Satoh, H., Ohkouchi, S. and Shibata, H. (2002) Structures, functions and molecular evolution of the penta-EF-hand Ca^{2+}-binding proteins. Biochim. Biophys. Acta **1600**, 51–60
24 Shibata, H., Suzuki, H., Kakiuchi, T., Inuzuka, T., Yoshida, H., Mizuno, T. and Maki, M. (2008) Identification of Alix-type and Non-Alix-type ALG-2-binding sites in human phospholipid scramblase 3: differential binding to an alternatively spliced isoform and amino acid-substituted mutants. J. Biol. Chem. **283**, 9623–9632
25 Bateman, A., Finn, R. D., Sims, P. J., Wiedmer, T., Biegert, A. and Soding, J. (2009) Phospholipid scramblases and Tubby-like proteins belong to a new superfamily of membrane tethered transcription factors. Bioinformatics **25**, 159–162
26 Santagata, S., Boggon, T. J., Baird, C. L., Gomez, C. A., Zhao, J., Shan, W. S., Myszka, D. G. and Shapiro, L. (2001) G-protein signaling through tubby proteins. Science **292**, 2041–2050
27 Mukhopadhyay, S. and Jackson, P. K. (2011) The tubby family proteins. Genome Biol. **12**, 225
28 Caberoy, N. B. and Li, W. (2009) Unconventional secretion of tubby and tubby-like protein 1. FEBS Lett. **583**, 3057–3062
29 Caberoy, N. B., Zhou, Y. and Li, W. (2010) Tubby and tubby-like protein 1 are new MerTK ligands for phagocytosis. EMBO J. **29**, 3898–3910
30 Merregaert, J., Van Langen, J., Hansen, U., Ponsaerts, P., El Ghalbzouri, A., Steenackers, E., Van Ostade, X. and Sercu, S. (2010) Phospholipid scramblase 1 is secreted by a lipid raft-dependent pathway and interacts with the extracellular matrix protein 1 in the dermal epidermal junction zone of human skin. J. Biol. Chem. **285**, 37823–37837
31 Simons, M. and Raposo, G. (2009) Exosomes-vesicular carriers for intercellular communication. Curr. Opin. Cell Biol. **21**, 575–581
32 Mathivanan, S., Ji, H. and Simpson, R. J. (2010) Exosomes: extracellular organelles important in intercellular communication. J. Proteomics **73**, 1907–1920
33 Cocucci, E., Racchetti, G. and Meldolesi, J. (2009) Shedding microvesicles: artefacts no more. Trends Cell Biol. **19**, 43–51
34 Shibata, H., Suzuki, H., Yoshida, H. and Maki, M. (2007) ALG-2 directly binds Sec31A and localizes at endoplasmic reticulum exit sites in a Ca^{2+}-dependent manner. Biochem. Biophys. Res. Commun. **353**, 756–763
35 Hirose, J., Kitabatake, N., Kimura, A. and Narita, H. (2004) Recognition of native and/or thermally induced denatured forms of the major food allergen, ovomucoid, by human IgE and mouse monoclonal IgG antibodies. Biosci. Biotechnol. Biochem. **68**, 2490–2497
36 Horii, M., Shibata, H., Kobayashi, R., Katoh, K., Yorikawa, C., Yasuda, J. and Maki, M. (2006) CHMP7, a novel ESCRT-III-related protein, associates with CHMP4b and functions in the endosomal sorting pathway. Biochem. J. **400**, 23–32
37 Havrylov, S., Ichioka, F., Powell, K., Borthwick, E. B., Baranska, J., Maki, M. and Buchman, V. L. (2008) Adaptor protein Ruk/CIN85 is associated with a subset of COPI-coated membranes of the Golgi complex. Traffic **9**, 798–812
38 Okumura, M., Ichioka, F., Kobayashi, R., Suzuki, H., Yoshida, H., Shibata, H. and Maki, M. (2009) Penta-EF-hand protein ALG-2 functions as a Ca^{2+}-dependent adaptor that bridges Alix and TSG101. Biochem. Biophys. Res. Commun. **386**, 237–241
39 Katoh, K., Shibata, H., Suzuki, H., Nara, A., Ishidoh, K., Kominami, E., Yoshimori, T. and Maki, M. (2003) The ALG-2-interacting protein Alix associates with CHMP4b, a human homologue of yeast Snf7 that is involved in multivesicular body sorting. J. Biol. Chem. **278**, 39104–39113
40 Nickel, W. and Rabouille, C. (2009) Mechanisms of regulated unconventional protein secretion. Nat. Rev. Mol. Cell Biol. **10**, 148–155
41 Merrick, B. A., Dhungana, S., Williams, J. G., Aloor, J. J., Peddada, S., Tomer, K. B. and Fessler, M. B. (2011) Proteomic profiling of S-acylated macrophage proteins identifies a role for palmitoylation in mitochondrial targeting of phospholipid scramblase 3. Mol. Cell Proteomics **10**, M110 006007
42 Trajkovic, K., Hsu, C., Chiantia, S., Rajendran, L., Wenzel, D., Wieland, F., Schwille, P., Brugger, B. and Simons, M. (2008) Ceramide triggers budding of exosome vesicles into multivesicular endosomes. Science **319**, 1244–1247
43 Valadi, H., Ekstrom, K., Bossios, A., Sjostrand, M., Lee, J. J. and Lotvall, J. O. (2007) Exosome-mediated transfer of mRNAs and microRNAs is a novel mechanism of genetic exchange between cells. Nat. Cell Biol. **9**, 654–659
44 Pisitkun, T., Shen, R. F. and Knepper, M. A. (2004) Identification and proteomic profiling of exosomes in human urine. Proc. Natl. Acad. Sci. U.S.A. **101**, 13368–13373
45 Mathivanan, S., Fahner, C. J., Reid, G. E. and Simpson, R. J. (2012) ExoCarta 2012: database of exosomal proteins, RNA and lipids. Nucleic Acids Res. **40**, D1241–1244

46 Subra, C., Grand, D., Laulagnier, K., Stella, A., Lambeau, G., Paillasse, M., De Medina, P., Monsarrat, B., Perret, B., Silvente-Poirot, S. et al. (2010) Exosomes account for vesicle-mediated transcellular transport of activatable phospholipases and prostaglandins. J. Lipid Res. **51**, 2105–2120
47 Mathivanan, S., Lim, J. W., Tauro, B. J., Ji, H., Moritz, R. L. and Simpson, R. J. (2010) Proteomics analysis of A33 immunoaffinity-purified exosomes released from the human colon tumor cell line LIM1215 reveals a tissue-specific protein signature. Mol. Cell Proteomics **9**, 197–208
48 Baietti, M. F., Zhang, Z., Mortier, E., Melchior, A., Degeest, G., Geeraerts, A., Ivarsson, Y., Depoortere, F., Coomans, C., Vermeiren, E. et al. (2012) Syndecan-syntenin-ALIX regulates the biogenesis of exosomes. Nat. Cell Biol. **14**, 677–685
49 Matsuo, H., Chevallier, J., Mayran, N., Le Blanc, I., Ferguson, C., Fauré, J., Blanc, N. S., Matile, S., Dubochet, J., Sadoul, R. et al. (2004) Role of LBPA and Alix in multivesicular liposome formation and endosome organization. Science **303**, 531–534
50 Nabhan, J. F., Hu, R., Oh, R. S., Cohen, S. N. and Lu, Q. (2012) Formation and release of arrestin domain-containing protein 1-mediated microvesicles (ARMMs) at plasma membrane by recruitment of TSG101 protein. Proc. Natl. Acad. Sci. U.S.A. **109**, 4146–4151
51 Kowalczyk, J. E., Beresewicz, M., Gajkowska, B. and Zablocka, B. (2009) Association of protein kinase C delta and phospholipid scramblase 3 in hippocampal mitochondria correlates with neuronal vulnerability to brain ischemia. Neurochem. Int. **55**, 157–163

Received 4 December 2012/15 January 2013; accepted 25 January 2013

Published as Immediate Publication 26 January 2013, doi 10.1042/BSR20120123

Biosci. Rep. (2013) / **33** / art:e00026 / doi 10.1042/BSR20120123

OPEN ACCESS

Original Paper

SUPPLEMENTARY DATA

ALG-2-interacting Tubby-like protein superfamily member PLSCR3 is secreted by exosomal pathway and taken up by recipient cultured cells

Tatsutoshi INUZUKA*, Akira INOKAWA*, Cen CHEN*, Kumiko KIZU†, Hiroshi NARITA†, Hideki SHIBATA* and Masatoshi MAKI*[1]

*Department of Applied Molecular Biosciences, Graduate School of Bioagricultural Sciences, Nagoya University, Furo-cho, Chikusa-ku, Nagoya 464-8601, Japan, and †Department of Food and Nutrition, Kyoto Women's University, 35 Kitahiyoshi-cho, Imakumano, Higashiyama-ku, Kyoto 605-8501, Japan

MATERIALS AND METHODS

Purification of anti-Scr3 mAb

Ascitic fluid (1 ml) was diluted with an equal volume of PBS (137 mM NaCl, 2.7 mM KCl, 8 mM Na_2HPO_4, 1.5 mM KH_2PO_4, pH 7.3) and loaded onto a 1-ml column of Protein G Sepharose. After washing the column with PBS, antibodies were eluted with 100 mM glycine–HCl, pH 3.0, and then the eluate was neutralized with Tris/HCl, pH 8.0, dialysed against TBS (10 mM Tris/HCl, pH7.5, 150 mM NaCl) and then stored in the presence of 0.02 % (w/v) NaN_3 at 4 °C or − 30 °C for long-term storage.

3D structure modelling

The 3D structure of Scr3 was predicted by two independent methods: (i) Swiss Model [1] at the following URL: http: //swiss-model.expasy.org/, where the 3D model of PLSCR1 predicted by Bateman et al. [2] (pdb file kindly provided by Dr Bateman) was used as a target, and (ii) Robetta Server using Ginzu [3] at the following URL: http://robetta.bakerlab.org/, where PDB code 1zxu was automatically selected as a homology target.

[1] To whom correspondence should be addressed (email: mmaki@agr.nagoya-u.ac.jp).

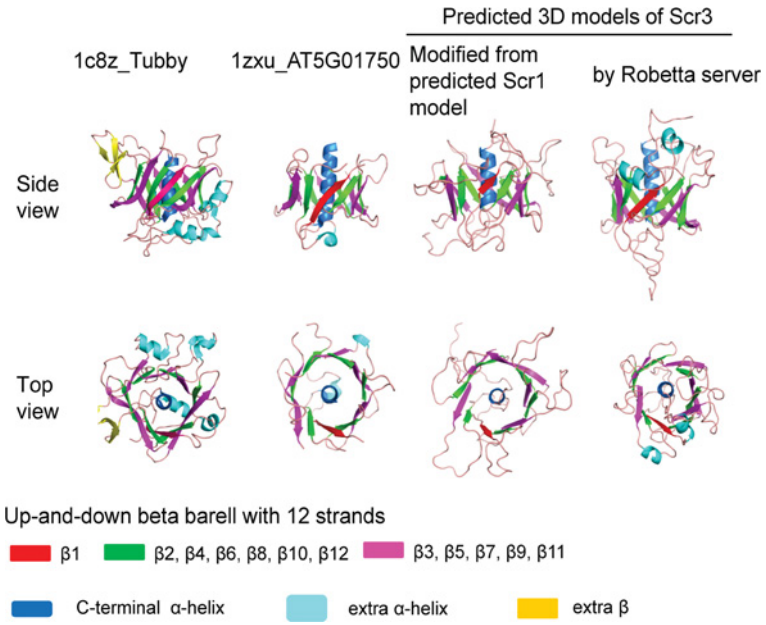

Figure S1 **Predicted structure of Scr3**

Two 3D structure models of Scr3 were obtained by Swiss Modeling based on the previously predicted structure of Scr1 and by Robetta server as described in the Supplementary Materials and methods, and they are shown by ribbon presentations from residues 60–285 (Swiss Modeling) or 60–295 (Robetta). Structures of Tubby and AT5G01750 were retrieved from Protein Data Bank (PDB ID, 1c8z and 1zxu, respectively). Secondary structures are shown in different colours as indicated. Each C-terminal helix (blue) is enclosed in a β barrel of 12 anti-parallel strands (β strand no. 1, red; odd nos., magenta; even nos., green).

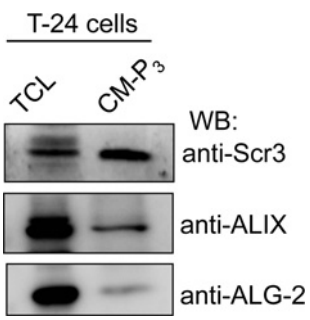

Figure S2 Exosomal secretion of endogenous Scr3 from human cells

Conditioned medium from human bladder carcinoma T-24 cells was centrifuged at 100 000 ***g*** for 60 min, and pellets (CM-P_3) as well as TCL were analysed by WB using respective antibodies as indicated.

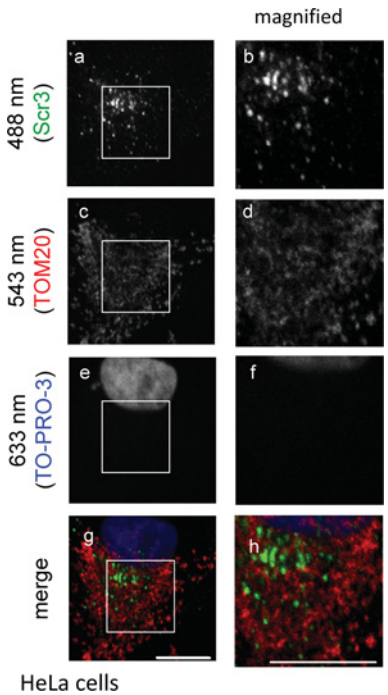

Figure S3 Non-mitochondrial subcellular localization of transiently expressed Scr3 in HeLa cells

HeLa SS4 cells were transfected with pIRE1neo/Scr3 that expresses WT untagged Scr3 and cultured on coverslips. After fixation, cells were permeabilized with 0.1% (v/v) Triton X-100 for 5 min and then immunostained with anti-Scr3 mAb and anti-TOM20 (a mitochondrial marker) pAb and stained with TO-PRO-3 for chromosomal DNA. The fluorescent signals of secondary antibodies, Alexa Fluor 488-conjugated anti-mouse IgG (excitation at 488 nm; a, b) and Cy3-labelled anti-rabbit IgG (excitation at 543 nm; c, d), and TO-PRO-3 (excitation at 633 nm; e, f) were analysed with a confocal laser-scanning microscope and are represented in black and white (a–f). Merged images are shown in colour (g, h) for Scr3 (green), TOM20 (red) and TO-PRO-3 (blue). Magnified views of the small boxes in a, c, e and g are shown in b, d, f and h, respectively. Bars, 10 μm.

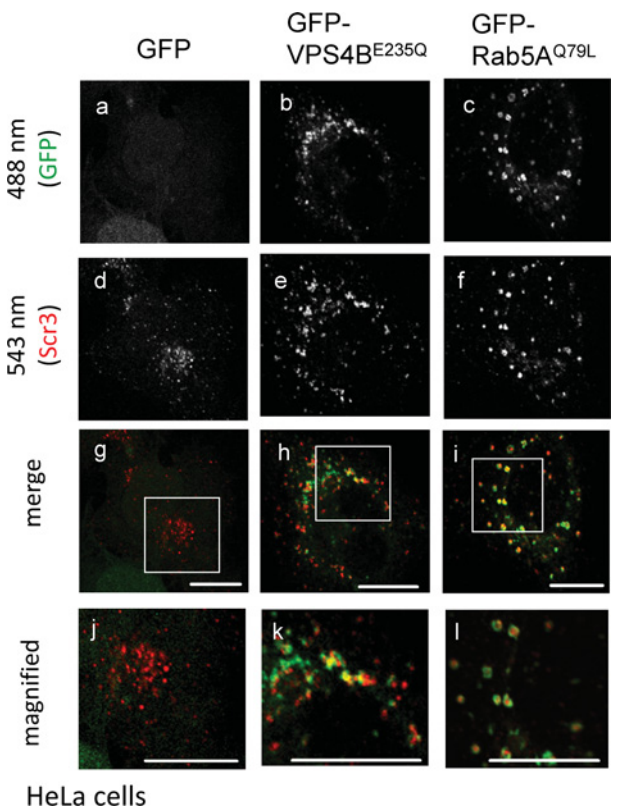

Figure S4 Effects of disturbance of endosomal membrane traffic on secretion of Scr3

HeLa SS4 cells were co-transfected with pIRE1neo/Scr3 and with expression plasmids for GFP-VPS4B^{E235Q} (b, e, h, k), GFP-Rab5^{Q79L} (c, f, i, l) or GFP as a control (a, d, g, j). One day after transfection, the cells were processed for immunocytochemistry using anti-Scr3 mAb and Cy3-conjugated goat anti-mouse IgG. Fluorescence signals of GFP (green; excitation at 488 nm; a, b, c) and Cy3 (red; excitation at 543 nm; d, e, f) were analysed with a confocal laser scanning microscope, and the images are represented in black and white (a–f). Merged images are shown in colour (g–i). Magnified views of the small boxes in g, h and i are shown in j, k and l, respectively. Bars, 10 μm.

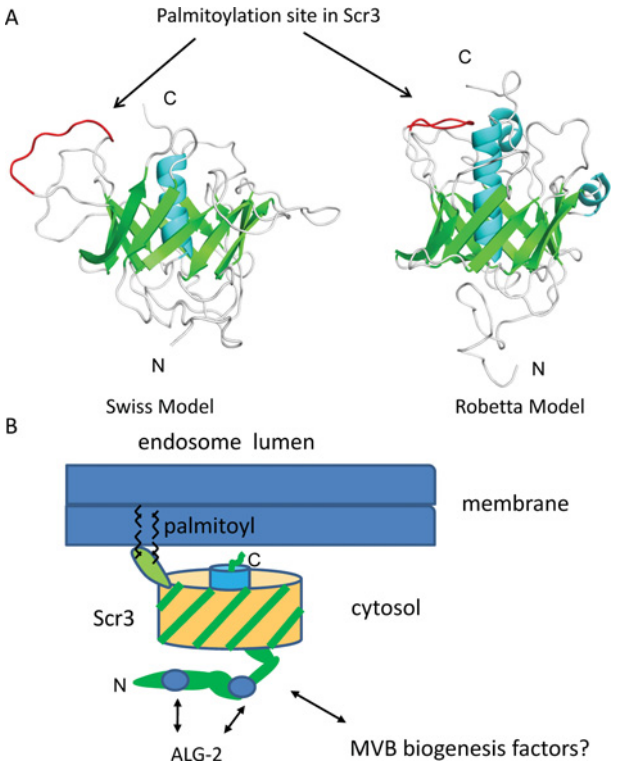

Figure S5 Palmitoylation site in Scr3 and membrane binding hypothesis

(**A**) Palmitoylation site (158-CGCSCCPC-165) is coloured in red in the loop between β_5 and β_6 of the predicted Swiss Model (left-hand panel) and Robetta model (right-hand panel). (**B**) A model of Scr3 binding to the lipid bilayer of endosomal membranes via palmitoyl moieties linked to the loop between β_5 and β_6 of the barrel. C-terminal α-helix is enclosed in the barrel and is not accessible to the membrane for integration. N-terminal flexible region has two binding sites for ALG-2 and probably contains binding sites for factors that are involved in MVB biogenesis.

Table S1 Primers used for PCR cloning

Construct	Type of PCR cloning	Primer orientation	Nucleotide sequence
pIRES1neo/SCR3_3CA	Step 1: overlapping 1	Forward	5′-GGAATTCAGTGGATCCATGGCAGGC-3′
		Reverse	5′-GCCTGCTGGTGCTGCGCTGCAACCACAGTGCAGCGGGCGGAGCAAAC-3′
	Overlapping 2	Forward	5′-GTTGCAGCGCAGCACCAGCAGGCCTCCAGGAGATGGAAGTACAGGCTC-3′
		Reverse	5′-GTTACTAGTGGATCCTGGTGGCCTC-3′
	Step 2: infusion	Forward	5′-GGAATTCAGTGGATCCATGGCAGGC-3′
		Reverse	5′-GTTACTAGTGGATCCTGGTGGCCTC-3′
pIRES1neo/SCR3_4CA	Site-directed mutagenesis	Forward	5′-CTGCACTGTGGTGCAAGCGCAGCACCAGCAGG-3′
		Reverse	5′-CCTGCTGGTGCTGCGCTTGCACCACAGTGCAG-3′
pScr3-GFP	Infusion	Forward	5′-GGACTCAGATCTCGAGCCATGGCAGGCTACTTGCC-3′
		Reverse	5′-CCGCGGTACCGTCGAATAACTGGTGACGGCAGAGGG-3′

REFERENCES

1 Arnold, K., Bordoli, L., Kopp, J. and Schwede, T. (2006) The SWISS-MODEL Workspace: a web-based environment for protein structure homology modelling. Bioinformatics **22**, 195–201
2 Bateman, A., Finn, R. D., Sims, P. J., Wiedmer, T., Biegert, A. and Söding, J. (2009) Phospholipid scramblases and Tubby-like proteins belong to a new superfamily of membrane tethered transcription factors. Bioinformatics **25**, 159–162
3 Chivian, D., Kim, D. E., Malmstrom, L. and Baker, D. (2005) Automated prediction of domain boundaries in CASP6 targets using Ginzu and RosettaDOM. Proteins **61** (Suppl. **7**), 193–200

Received 4 December 2012/15 January 2013; accepted 25 January 2013

Published as Immediate Publication 26 January 2013, doi 10.1042/BSR20120123